Hot Spots on Io: Initial Results from Galileo's Near Infrared Mapping Spectrometer

Rosaly Lopes-Gautier, A. G. Davies, R. Carlson, W. Smythe, L. Kamp (Jet Propulsion Laboratory, California Institute of Technology, Pasadena, CA 91109), L. Soderblom (U.S. Geological Survey, Flagstaff, Arizona), F.E. Leader, R, Mehlman (Institute of Geophysics and Planetary Physics, University of California, Los Angeles) and the Galileo NIMS Team.

Abst ract. The Near-Infrared Mapping Spectrometer on Galileo has monitored the volcanic activity on 10 since June 28, 1996. This paper presents preliminary analysis of NIMS thermal data for the first four orbits of the Galileo mission. NIMS has detected 18 new hot spots and 12 others which were previously known to be active. The distribution of the hot spots on Io's surface may not be random, as hot spots surround the two bright, SO_2-rich regions of Bosphorus Regio and Colchis Regio. Most hot spots seem to be persistently active from orbit to orbit and 10 of those detected were active in 1979 during the Voyager encounters. We report the distribution of hot spot temperatures and find that they are consistent with silicate volcanism.

Introduction

The Near-Infrared Mapping Spectrometer (MMS) is investigating the composition of Io's surface, the distribution of SO_2 on the surface [Carlson et al. 19971, and the distribution and temporal variability of hot spots on the surface. This paper presents the results of our search for new and recurrent hot spots on Io from observations taken during Galileo's first four orbits; the distribution of these hot spots on the surface, and an analysis of hot spot temperatures using a nightside observation taken during the first orbit. We use the term hot spot to denote an active, or recently active, volcanic region on Io, recognized by the observation of thermal emission significantly above the NIMS detection limit of 180 K [Smythe et al. 1995], which in turn is significantly above Io's passive background temperatures (107 K to 124 K for noontime equatorial temperatures, McEwen et al. 1992a,b). Preliminary analysis of NIMS data from several orbits shows that the single temperature that best fits the NIMS data for any given hot spot can vary significantly from orbit to orbit [Lopes-Gautier et al., 1997]. This is to be expected given that the level of activity at each volcanic region can vary with time and can include periods of quiescence.

Instrument and observations

The NIMS instrument has been described previously by Carlson et al. [1992] and Smythe et al. [1995]. NIMS spans the wavelength range 0.7 to 5.2 microns and thus measures reflected sunlight and thermal emission. The instrument includes a spectrometer with a scanning grating. NIMS forms spectra with the moving grating in combination with 17 detectors. The 17 wavelengths obtained for each grating position are acquired simultaneously, thus providing a "snapshot" of the target Spectra obtained for different grating positions may not be of precisely the same spot on the planet, because of motion of the field of view relative to the surface during the time between grating steps (0,33 seconds), The consequences of this motion are further discussed in section 5.

NIMS has observed Io several times per orbit during Galileo's orbits G 1 through E4 (see table 1 for dates). Most observations were taken at ranges between 244,000 and 860,000 km (corresponding to spatial resolutions of 122 to

430 km/NIMS pixel). The observations cover all latitudes and most cover the whole disk, with a few targeting only part of the disk. The number of wavelengths returned varies from 102 to 408. The NIMS Io observing plan has been described by Smythe et al. [1995].

Detection of Hot Spots

The positions of hot spots observed by NIMS in orbits G l through E4 are listed in Table 1. A pixel-by-pixel hot spot search was carried out on each observation, A pixel was considered to contain a hot spot when the positive slope of the spectrum between 3.5 and 5 microns was greater than that of all surrounding pixels. It is important to note that these areas do not represent all of the thermal emission that NIMS detects from Io. Nightside observations show other NIMS pixels that have significant thermal output based on their positive slope between 3 and 5 microns, but these were not selected as hot spots because either (i) the local maximum was less than 5% greater than that of the surrounding pixels or (ii) the pixels had less output than neighboring pixels which were identified as hot spots. The first case may represent hot spots which are either very small or cool. The second case may represent adjacent hot spots that cannot be resolved at the available spatial resolution, or energy that is distributed between pixels because of the instrument's point-spread function [Carlson et al. 1992]. Our temperature-area calculations (section 5) show that all of the hot spots identified so far are sub-pixel at NIMS spatial resolutions.

The latitudes and longitudes listed in Table l are taken as the central coordinates of the NIMS pixels containing each hot spot. Limb tits were done to the NIMS observations so that the projected coordinates were as accurate as possible, but errors of half a NIMS field of view (i.e. half the pixel size) can be expected and are listed in Table 1. The coordinates derived from the highest spatial resolution observation available for each hot spot were considered to be the moat accurate. Greater precision in locations can be obtained from observations by the Solid State Camera (SS1), provided that the hot apot temperatures are sufficiently high to be detectable in their images [McEwen et al. 1997].

Distribution of hot spots on the surface

The 30 hot spots detected by NIMS (Table 1) are shown superimposed on a mosaic of Voyager images (Fig. 1). Of these, 18 are new, 10 were known from Voyager data as either hot spots or plume sites [e.g. Strom and Schneider 1982; Pearl and Sinton 1982; McEwen et al. 1989], and 2 had been discovered from ground-based observations [Spencer et al. 1997].

Most of the new hot spots detected by NIMS (15 out of 18) are located in the anti-Jovian hemisphere (centered on. longitude 180 W), for which Voyager IRIS provided sparse coverage [McEwen et al. 1989]. The spatial resolution of NIMS observations is lower on the Jupiter-facing hemisphere, centered on longitude O (Fig. 1), and so far 9 hot spots detected by Voyager on that hemisphere have not been detected by NIMS. These Voyager-detected hot spots are Amaterasu, Creidne, near Nemea Planum, Mazda Catena, Aten Patera, Viracocha Patera, Mbali Patera, Svarog Patera, and an unnamed volcanic center at 335W, ION [McEwen et al. 1989, 1992]. The Voyager hot spots Ulgen and Babbar Patera are probably seen as a single hot spot by NIMS ("West of Pele" in Table 1) because of the low spatial resolution in the currently available observations. NIMS observations in future orbits will provide higher spatial resolution for the Jupiter-facing hemisphere and we expect that NIMS will detect the "missing" Voyager hot spots if they are still active.

The distribution of hot spots in Fig. l is biased in favor of lower latitudes. The sub-spacecraft point for all observations is nearly equatorial and therefore hot spots at higher latitudes (particularly over 4S degrees) are harder to detect as spatial resolution decreases. Closer flybys of Io, including a polar pass scheduled near the end of the mission in 1999, will provide the best opportunities for detecting hot spots at higher latitudes.

The hot spot distribution in Fig. 1 may not be random. A circular pattern is shown by the hot spots surrounding the bright region of Bosphorus Regio (centered at about 120 W, 3 S), and a similar though less obvious circular pattern around the Colchis Regio region (centered at about 200 W, O). Both regions are thought to be SO_2-rich topographic basins [Gaskell et al. 1988, McEwen et al. 1995]. The hot spot distribution around Bosphorus Regio is particularly striking, with at least 9 hot spots found so far surrounding the 1,600 km diameter basin (Fig. l). Furthermore, the NIMS G1 nightside data show that the center of this basin has no thermal output which was detectable by NIMS in the 3 to 5 micron region, while the pixels in the "ring of tire" defined by the hot spots surrounding the basin have a signal significantly above the noise level, as shown in the 5-micron image of the observation (Fig. 2). This indicates that areas of enhanced thermal emission are present around the basin, but not in its center.

Temperatures and areas of hot spots from NIMS nightside data

NIMS data can be fitted to a Planck fiction to yield a best-tit black body temperature for the spectra from each pixel. This is a relatively straightforward procedure using nightside data (see Davies et al. 1997 for a description of the temperature-fitting algorithm). Dayside data includes a component from reflected sunlight which must be removed or accounted for before the data can be fitted, Most NIMS observations view Io's dayside, the geometry predominantly available when the spacecraft reaches its closest approach to Io in each orbit. AU data used in the following analysis were from a nightside observation (Fig. 2) in the first Galileo orbit. This observation was taken in 408 wavelengths at a spatial resolution of 350 km/NIMS pixel.

We have analyzed the spectra for 14 hot spots detected in this observation. To minimize the effect of the instrument's point-spread function, we summed two adjacent pixels in the scan mirror direction. To minimize the effects of image motion during spectrum acquisition, we fit each of 24 sub-spectra (which consist of 17 wavelengths across the 1 to 5 micron region sampled simultaneously) to a Planck function to derive a single-temperature fit. The temperatures obtained from each sub-spectra were then averaged. The average temperature for each hot spot is shown in Table 2, together with the standard deviations yielded by this method. The temperatures range from 384 ± 10 K to 606 ± 34 K. Equivalent areas were calculated using the average temperature for each hot spot and the flux contained in the two summed NIMS pixels. Areas were corrected for viewing angle. Errors on areas were taken to be proportional to the standard deviations in the corresponding temperatures.

The procedure used here for deriving color temperatures consistently underestimates temperatures relative to an alternative procedure which does not sum pixels and which selects the pixel with the highest apparent thermal output. Comparison of results obtained using both methods show that the average temperatures obtained for each hot spot using a single pixel were greater than those using summed pixels, with the differences ranging from O K up to 80 K, with most being under 30 K. Comparing the results, we consider that the choice of procedure may contribute up to an additional 50 K uncertainty to the positive boundary of the format errors reported in Table 1. We selected the procedure of summing most being under 30 K. Comparing the results, we consider that the choice of procedure may contribute up to an additional 50 K uncertainty to the positive boundary of the formal errors reported in Table 1. We selected the procedure of summing over the point-spread function as the most accurate because it minimizes errors arising from uncertainties of location of a hot spot within a NIMS pixel. The areas given in Table 2 show that hot spots are 0.2% or less of the area of a NIMS pixel.

Although a single temperature tit is a simplistic approach, and two-temperature fits can be done using NIMS data [Davies et al. 1997], single temperatures are extremely useful for comparison with Voyager and ground-based results (Table 2). They cart also serve as a basis for intercomparison of NIMS data from orbit to orbit and from several observations within the same orbit, in order to monitor temporal variations in activity at scales from hours to months. Single-temperature tits wiU, however, be biased towards the temperature of the cooler component of a two-temperature fit, given that typically the cooler component is much larger in area [e.g. Crisp and Baloga 1990] and its signature dominates the NIMS wavelength region. Therefore, the values in Table 2 significantly underestimate the temperature of the hotter (liquidUs) component, as shown by Davies et al. [1997] for the Zamama (S. Volund) hot spot. Given that most of the temperatures in Table 2 are higher than 500 K, too high for elemental sulfur alone, and that they underestimate the temperature of the liquidus component, the NIMS results are consistent with silicate volcanism being the predominant type on 10.

Results and Conclusions

This first-order analysis shows that the NIMS data arc of prime value to the study of Io's volcanic activity. The highlights from this analysis can be summarized as:

(i) Detection of new hot spots and their distribution on the surface 18 new hot spots were detected by NIMS during preliminary analysis of data from the first four orbits in the Galileo tour. All hot spots detected so far have been within 50 degrees of latitude from the equator. Hot spots at higher latitudes, if they exist, may not be easily detected by NLMS during the Galileo tour due to the nearly equatorial view of observations. The distribution of hot spots around two SO_2-rich equatorial regions, Bosphorus Regio and Colchis Regio, may reflect a concentration of volcanic vents arranged around these regions, which are thought to be topographic basins. However, this distribution has not yet been tested for randomness. Bosphorus Regio shows a particularly striking distribution of hot spots as a "ring of fire". A detailed NIMS thermal map of the area is needed to confirm the preliminary observation that the center of this basin is a cold area (below detectability limit of 180 K), surrounded by pixels containing individual hot spots and other areas of thermal anomaly.

(ii) Assessment of persistency in the activity of hot spots: NIMS data from the first 4 orbits, together with Voyager and ground-based data, show that the majority of hot spots on 10 are persistently active. Out of the 30 hot spots detected to date by NIMS, 10 had been observed by Voyager in 1979 as active volcanic areas and 2 bad been discovered since from ground-based observations [Spencer and Schneider 1996; Spencer et al. 1977]. New hot spots detected by NIMS have been seen as active in more than one orbit, with the exception of two (Zal and Fo) though the lack of detection could be due to a temporary waning in activity rather than a total shut-off. The same could have happened to the hot spots in Colchis (at 191 W, +28) and in Reiden Patera detected by SS1 in the G 1 orbit [McEwen et al. 1997] which have not yet been detected by NIMS. Our results indicate that most hot spots on 10 may been available on the temperatures of these hot spots, Given the uncertainties in temperature and area models, the differences between values obtained from Voyager IRIS and from NIMS data cannot be considered significant, Preliminary temperature calculations from dayside NIMS data from orbit G2 [Lopes-Gautier et al. 1997] show that the Malik Patera hot spot increased in temperature by at least 400 K in the two months since orbit G 1. NIMS hot spot data from orbit G2 and beyond include hot spots, such as Loki, for which long-term monitoring has been available from ground-based observations [e.g. Veeder et al. 1994]. NIMS-derived temperatures will be a particularly useful contribution to the volcanic history of these hot spots. **Future work from NIMS Io darta will include:** (i) searching for correlations between hot spot temperature and chemistry, (ii) completing the longitudinal coverage and mapping the distribution of hot spots over the whole globe, (iii) directly comparing results from nightside and dayside data to assess temporal changes in hot spot temperature on timescales of hours (possibly minutes) to days, (iv) making global thermal maps to the limit of NIMS detectability, and (v) correlating hot spot detections by MMS with those from ground-based telescopes and from Galileo's SS1 experiment.

Acknowledgements: We thank E. Barbinis, J. Hui, P. Herrera. M. Segura, and J. Shirley for sequencing support; two anonymous referees for their reviews; and Dennis Matson, Alfred McEwen, and Haraldur Sigurdsson for their helpful comments. The Galileo Project is funded by the Nasa Solar System Exploration Division The work described here was performed at the Jet Propulsion Laboratory, California Institute of Technology, under contract with NASA.

References:

Carlson, R. W., W.D. Smythe, R. Lopes-Gautier, et al. The Distribution of Sulfur Dioxide and Other Infrared Absorbers on the Surface of Io in 1997. *Geophys. Res. Lett., this* issue.

Carlson, RW., P.R. Weissman, W.D. Smythe, et al. Near Infrared Spectrometer Experiment on Galileo. *Space Sci. Rev., 60,* 4S7-502, 1992.

Crisp. J. and S. Baloga. A method for lava flows with two thermal components, *J. Geophys. Res.,* 95, 1255-70. 1990.

Davies, A. G., A.S. McEwen, R Lopes-Gautier, et al. Temperature ● nd Area Constraints of the S. Volund Volcano on Io from the NIMS ● nd SSI instruments during the Galileo G1 orbit. *Geophys. Res. Lett.,* 1997, this issue.

Gaskell R. W., Synnott, S. P., McEwen, A. S., and Schaber, G. G.: Large-scale topography of Io: implications for internal structure end heat transfer. *Geophys. Res. Lett.,* 15, S81.584.

Lopes-Gautier, R. et al. *Lunar Planet. Sci.* Con~XXW/,p.831, 1997.

McEwen, AS. SO2-Rich Equatorial Basins and Epeirogeny of Io. *Icarus,* 113, p. 415-422, 1995.

McEwen, AS., J.I. Lunine, M.H. Cam. Dynamic Geophysics of Io. *NASA Special Publication 494,* pp. 11-46, 1989.

McEwen, A- S., et al. High temperature hot spots seen by Galileo's Solid State Imager (SS1) Experiment. *Geophys. Res. Mt.,* t997, this issue.

McEwen, A.S., N.R. Isbell, K.E. Edwards, and J.C. Pearl. New Voyager 1 Hot Spot Identifications and the Heat Ftow of Io. *Bull. Am. Astron. Soc. 24,* p.935, 1992a.

McEwen, A. S., N.R. Isbell, J.C. Pearl. Io thermophysics: new models with Voyager 1 thermal IR spectra. *Lunar Planet. Sci. Conference ,%XI/I, 881,* 1992b.

Pearl, J. and W.M. Sinton. Hot Spots of Io. In Morrison (Ed.) *Satellites of Jupiter,* Univ. Ariz. Press, p.724-755, 1982.

Smythe, W. D., R Lopes-Gautier, A. Ocampo, et al Galilean Satellite Observation Plans for the Near-Infrared Mapping Spectrometer on the Galileo Spacecraft *Jour. Geophys. Res., 100,* pp. 18,957-18,972, 1995.

Spencer, J.R. and N.M. Schneider. Io on the Eve of the Galileo Mission. Annu. Rev. *Earth Planet. Sci.,* 24, pp. *125-190.* t 996.

Spencer, J. R., J.A. Stansbery, C. Dumas, et al. A History of High-Temperature Volcanism, February 199S to May 1997. *Geophys. Res. Lett.,* 1997, this issue.

Spencer, J.R. and N.M. Schneider. 10 on the Eve of the Galileo Misaim Annu Rev. *Earth Planet. Sal., 24.* pp. *125-190, 1996.*

Spencer, J. R., J.A. Stansbery, C. Dumas, et al. A History of High-Temperature Volcanism. February 199S to May 1997. *Geophys. Res. Lett.*, 1997, *thin* issue.

Strom, R.G. and N.M. Schneider. Volcanic Eruption Plumes of Io. In Motion (Ed) *Satellites of Jupiter,* Univ. Ariz. Press, p. 598-633, 1982.

Veeder, O. et al. Io's Heat Ftow from Infrared Radiometry: 1983-1993. *J. Geophys. Res., Planets, vol. 99,* 17,095-17,162, 1994

R Lopes-Gautier, A.G. Davies, R.W. Carlson, W.D. Smythe: JPL, MS 183-601, Pasadena, CA 91109 (rlopes@issac.jpl.nasa.gov, ● gd @kookaburra.jpl.nasa.gov, rcarlson @issac.jpl .nasa.gov, wsmythe @issac.jpl.nasa .gov). L. Kamp: JPL, MS 168-514, Pasadena, CA 91109 (kamp@issac.jpl. nasa.gov). L. Soderblom, Branch of Astrogeologic Studies, U.S. Orological Survey. Flagstaff, AZ 86001 (lsoderblom @flagmail.wr. usgs.gov). F.E. Leader and R Mehlman, Institute of Geophysics and Planetary Physics, University of California, Los Angeles, CA 90095 (fleader@igpp.ucla.edu, rmehlman @igpp.ucla.edu).

(Received April 7. 1997, 1997; revised August 21, 1997; ● ccepted: September 10, 1997)

Table 1: Hot Spot Locations From G1 through E4

Name	W. Long	Lat	First NIMS Detection	Other Detections
Janus	42 ± 5	48 * 5	0 1	Ground-observed, SS1 (S4)
Hi'iaka	76 ± 4	1S ± 4	0 1	Ground-observed, NIMS C3
Zal	78 ± 10	43N ± 7	G1	
Oiah Bar	89 ± 5	16N ± 4	01	NIMS C3, SS1 E4
Sigurd	1 0 0 * 4	5S ± 4	G1	NIMS C3
Monan	106*4	19N ± 3	01	NIMS 02, NIMS C3
Altjirra	108 ± 4	33S ± 4	0 1	NIMS C3
Amirani	112*4	27N ± 4	01	Voyager, NIMS 02, C3
Maui	122 ± 3	19N ± 3	0 1	Voyager, NIMS G2, C3
Malik	1 2 7 * 3	35S ± 3	G1	NIMS 02, NIMS C3
Tupan	1 4 1 * 3	17S ± 3	01	NIMS 02, NIMS C3
9606W	147 ± 6	36N ± 6	0 1	NIMS C3
Prometheus	155 ± 3	1S ± 3	0 1	Voyager (plume), NIMS 02, C3
Culann	1 6 3 * 3	18S ± 3	01	NIMS 02, C3
Zamama	1 7 3 * 3	21N ± 3	G1	SSI G1, NIMS G2, C3, E4
Volund	174 ± 3	25N ± 3	C 3	Voyager. Possibly merged with S. Volund in NIMS G1, 02, and E4
Aidne	178 ± 3	2 5 * 3	0 1	NIMS 02, C3, E4
Fo	191 ± 3	39N ± 3	C3	
Sethlaus	1 9 5 * 3	50S ± 3	C3	NIMS E4
Rata	199*3	355*3	C3	NIMS E4
Lei-Kung	206±3	37N±3	C3	SS1 01 ground-observed
Isum	207 ± 3	31N ± 3	0 1	Voyager. SS1 01, NIMS 02, C3, E4
Marduk	212 ± 3	26S ± 3	0 2	Voyager (plume), SSI 01, NIMS C3, E4
9611A	218 ± 3	2S ± 3	C3	NIMS E4
Kurdalagon	219 ± 3	47S ± 3	C3	NIMS E4
Mulungu	219 ± 3	17N ± 3	0 2	SS1 01, NIMS C3, E4
Pillan	244 ± 3	13S ± 3	G 2	NfMS C3, E4
Pele	255 ± 3	20S ± 3	G 2	Voyager, ground-observed, SS1 01, C3 and E6, NIMS C3, E4
Daedalus	281*6	18N ± 3	E4	Voyager
W. Pele	283 ± 8	37S ± 4	0 2	Voyager (Babbar/Ulgen), NIMS C3, E4
Loki	309 ± 7	9N ± 7	G2	Voyager, ground-observed. NIMS E4, SS1 E6

TABLE 1: Locations of hotspots and other detections. The hotspot designations 96011A and 9606W are from John Spencer (pers. comm.). Voyager information is from Pearl and Sinton [1982], Strom and Schneider [1982], McEwen et al. [1989, 1992]. Correlation with SSI observations were based on McEwen et al. [1997]. Ground-based data are from Spencer et al. [1997] and Spencer and Schneider [1996]. Dates for the NIMS observations, all in 1996, are: June 28 (O 1), September 7 (G2), November 6 (C3), and December 18 (E4).

Table 2: Hot Spot Measurements From G 1

NAME	T (K)	AREA (km²)	Other measurements
Hi'iaka	459 ± 24	32 ± 2	
Zal	494 *23	40*2	
Gish Bar	48s * 19	15*1	SS1 hot spot in S4. temperature for hot component T>825K [McEwen et al., 1997]
Sigurd	434*3 I	30*2	
Monan	560*20	8 ± 0.3	
Altjirra	384* 10	192 ± 5	
Amirani	550 ± 41	29 ± 2	voyager hot spot,
Maui	508 ± 14	11 ± 0.3	T=395K, A-531 km² or T=200K, A=7543 km².Pearl end Sinton [19S2]
Malik	578 ± 20	7* 0.2	
Tupan	606*34	6* 0,4	
9606W	458 ± 37	11*1	
Prometheus	574 *29	3 * 0.2	
Culann	517 ± 15	18 ± 0.5	
Zamama	537 ± 34	16 ± 1	SS1 hot in G1, NIMS/ SS1 two-component fit, T=450K and T-l 100K [Davies et al. 1997].

Figure 2: Io observed by NIMS 00 June 28. 1996, et UTC=17:17:23, covering longitudes 46W to 183W. Observation name is G1INNSPEC01. This 5-micron image shows oft of the disk in darkness, except for the westernmost region which was sunlit. Several hot spots are labelled. Tbe dark region near the center of the disk is the center ofBosphorus Regio, it is surrounded by hot spots and other pixels which appear bright at 5 microns and may contain thermal anomalies.

Figure 1: Distribution of the hot spots detected by NIMS on Io. The scale at the bottom shows the beat spatial resolution ● vailable so far from NIMS observations.

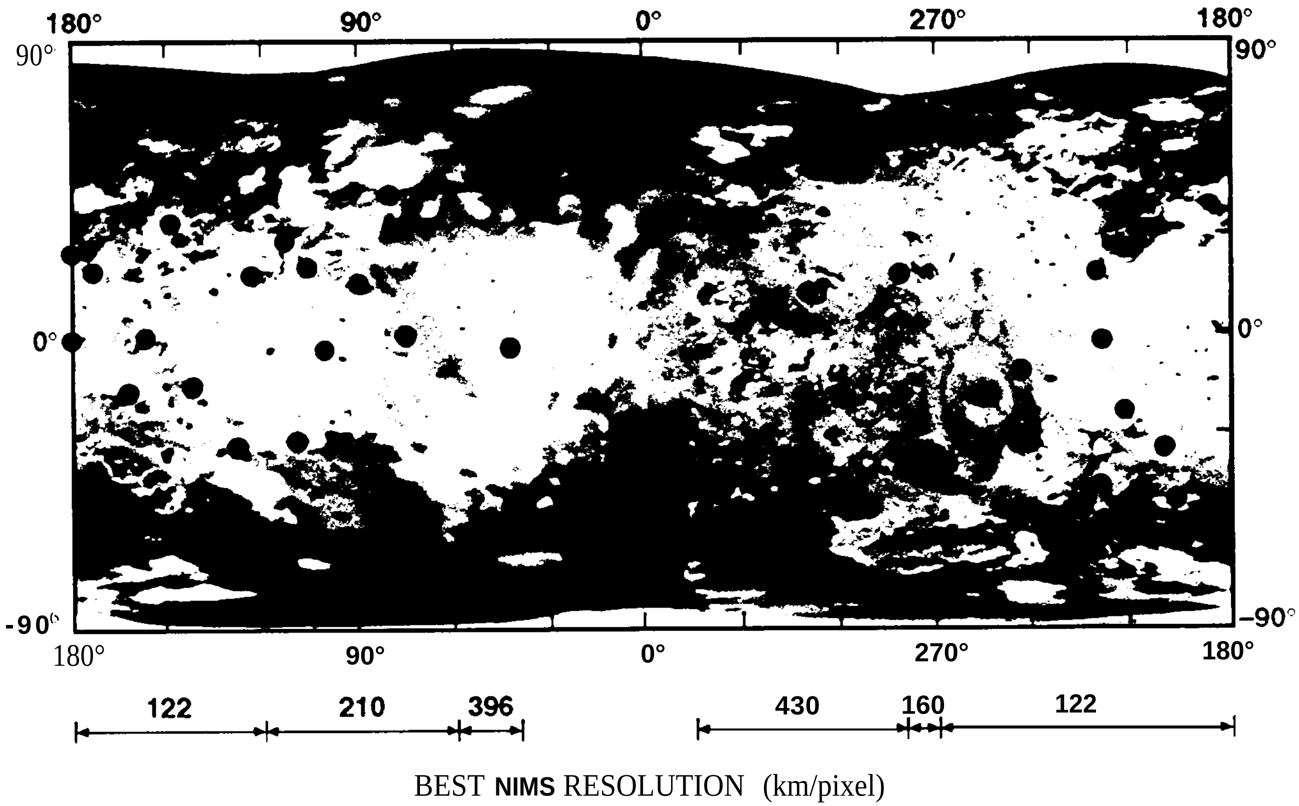
180°
90°
0°
270°
180°
90°
0°
-90°
90°
0°
-90°
180°
90°
0°
270°
180°
122
210
396
430
160
122
BEST NIMS RESOLUTION (km/pixel)

Fig 8

Fig 2